International Journal of Environmental Sciences
ISSN: 2229-7359
Vol. 11 No. 21s, 2025
https://theaspd.com/index.php

Modelling And Optimization Of Alumina & Silica Reinforced Magnesium Metal Matrix Composite Using RSM BBD Approach & ANOVA For Quantitative Parameters

Dheeraj Kumar[1], **Rajesh Kumar Porwal**[2]
[1]Research Scholar, Faculty of Mechanical Engineering, Institute of Technology, SRMU Lucknow, U.P., India
[2]Faculty of Mechanical Engineering, Institute of Technology, SRMU, Lucknow, U.P., India
[1]dheerajkr18@gmail.com,[2]porwal.me@srmu.ac.in

Abstract
This paper explains the optimization of quantitative parameters for thermoelectric machining of magnesium based metal matrix composite. Sample prepared by stir casting method using Al_2O_{3p} (3%wt) and SiC_p (6%wt) as reinforcement. CNC wire cut EDM used for machining as per DoE developed using RSM-BBD approach. Input parameters Pulse on, pulse off time, current and wire speed was varied to obtain machining efficiency and surface quality. Experimental models are developed and justified by ANOVA for optimization and response plots depicting optimized parameters of higher metal removal rate and lower roughness. Current and wire speed played significant role in obtaining the optimum values of input parameters. Higher value of MRR is obtained at T_{on}=18µs, T_{off}=7µs, I=1A & WS=10.40m/sec while lower value of roughness is obtained at T_{on}=6µs, T_{off}=7µs, I=1A & WS=6.76m/sec. DoE based RSM-CD approach for multi objective optimization depicts combination of optimal input parameters T_{on}=6µs, T_{off}=5µs, I=1.2A & WS=10.4m/sec for high MRR (0.153128 mm^3/sec) and lower surface roughness (Ra=2.98165µm).

Important Terms: *Hybrid Composite, Wire-EDM, ANOVA, Stir Casting, Alloy AZ91, MRR, Magnesium Metal Matrix Composite (MMMC), RSM-BBD Approach, Surface Roughness.*

Abbreviations & Symbols:
MMMC- Magnesium Metal Matrix Composite; WEDM- Wire Electro Discharge (Erosion) Machining;
ANOVA- Analysis of Variance; RSM- Response Surface Methodology; Material Removal Rate- MRR; BBD- Box Behnken Design; Pulse-off-Time- T_{off}; Pulse-on-Time- T_{on}; Wire Speed- WS; Surface Roughness- SR or R_a; Current- I

1.0 INTRODUCTION

Composites are coherent blend of two or more substances. In its expansive form, it comprises one as a basis with additional elements as strengthening. Composites are engineered substances formed by amalgamating two or many different elements, each with distinct features, which yield enhanced characteristics when integrated [1 & 2]. It consists of a grid layer including metal-like substance, metals in strand or granules, and ceramic flecks or oxides serving as reinforcement. The material phases, despite being insoluble, demonstrate robust stickiness at their boundaries. It offers better properties that are difficult to obtain separately with metals, ceramics, or polymers [3].

Absolute magnesium possesses a restricted spectrum of uses because of its tendency to react and outdoors oxidation. Mg alloys and composites have a variety of uses and are lightweight while displaying remarkable qualities. Following steel and aluminium as the most often utilised structural metals, magnesium comes in third. Magnesium-based alloys and composites exhibit several notable properties, including low density, lower heat capacity, good damping capacity, excellent castability, effective elastic shielding, non-magnetism, satisfactory thermal conductivity, high durability, negative electrochemical potential, and they are both non-toxic & recyclable [4].

WEDM is an electro thermal mechanism, in which particles are stripped away from the specimen by sparks that follow one another between the component being worked on and the wire terminal in a di-electric liquid-based environment. The wire is not brought into interaction with the component being worked on during this operation. Dielectric fluid is used to wash the tiny bits aside. Material of wire can be copper, tungsten, brass, steel core wire or molybdenum. It might be diffused annealed or plated [27-29].

Mg casting is extensively utilised among respectable automakers as Ford, General Motors, Toyota & Volkswagen. The gear box housings, cross car beam, steering components, vehicle doors and radiator supports are typical automobile applications. The material's yield potency decreases with stiffer reinforcement but increases when the compositional percentage of SiC particles increases [5-13]. Environmentalists and lawmakers are pushing the automotive sector to create lighter, more efficient, and fuel-efficient vehicles. It aims to draw attention to the use of alloys and magnesium.

Kumar A. & co-authors, has evolved AZ91 centered composite element through diverse formulations of SiC using negative pressure enabled rotatory casting approach. They found that untainted alloys possess greater ductility than all established composites, and that unalterable tensile strength elevates with the proportion of granular reinforcements. Additionally, he listed the reasons why adding flux during casting is inappropriate [4]. Granular reinforcing can significantly increase a firmness and durability of magnesium alloy at a variety of temperatures [14-16]. Metallic substrate, ceramic grains and CNTs are popularly being utilized as reinforcements for magnesium alloy composites. Carbides of silica, Al_2O_3, carbides of titanium, Oxides of magnesium and other ceramic bits are highly acclaimed reinforcing agents [17-21].

I balasubramanian et al. fabricated AZ91D matrix composites with Carbides of silica as reinforcement ranging by weight (0 – 9%) through squeeze casting approach. A CNC lathe was used to grind down the established prototypes followed by tests for hardness, surface quality and MRR. Feeding rate & speed have a major impact on the degree of roughness. The degree of additives in magnesium blends diminishes the degree of surface roughness [22]. V. Kavimani and co-authors has maximized the wire cut machining variables (T_{on}, T_{off} & WF rate) for MRR and R_a of recently created composite made of magnesium with graphene & S_iC like additional agent by Taguchi-Grey Relational Analysis. On the basis of the Taguchi-grey relational grade values, the optimal level of the input process parameters is identified. Because of this, the parameters of the procedure were found to be P_{on} = 40ms, P_{off} = 23ms, D% = 10, Wire feed = 2 meter/minute, weight percent = 0.2 has given desired results [23].

L. Arunkumar & B. K. Raghunath has prepared the sample by powder metallurgy method and examined the influence of electrical current, pulse on time, and pulse off time on the material extraction rate and tool wear rate of Mg/SiC_p composites composed of metal matrix while electric discharge machining. The top current flow of 10 Amps with pulse on & pulse off times of 1000μs and 20μs As a consequence the material removal rate reaches its outmost value. Similar to the maximum, the lowest was reached at 5 Amps with pulse on and off times of 200μs and 50μs, respectively. The greatest and minor tool wear rates are noted at the currents of 5A and 10A, correspondingly, with pulse on time and pulse off time of 600μs and 125μs and 200μs and 50μs, consequently [24].

Gopal P. M. and others optimized Wire electro discharge machining constraints T_{on}, T_{off} and Wf while processing of developed BN/Mg/CRT blended composites to get degree of smoothness & MRR. They have utilised additives ranging between 5 & 10% by weight with 2% of BN. Superior exterior finish is acclaimed by reduced reinforcement proportion & size, P_{on}, Wf, and high side of P_{off}, yet superior MRR is acclaimed by lesser additives %, reinforcement proportions, P_{off}, excessive P_{on}, and Wf [25].

S. Samanta and coauthors studied the WEDM parametric effects on Mg-SiC metallic composites alongside 5% additives in dusty structure. Accounting 6-constraints namely T_{on}, T_{off}, di-electric flushing pressure, $V_{breakdown}$, I_{max} and servo feed for the assessment on MRR and exterior roughness employing RSM technique. The most vital role acclaimed for the MRR and SR, respectively, were testified to be P_{on} and P_{off}. [26].

Bekir Yalcin & others explored the influence of WEDM factors T_{on}, T_{off} and V_{servo} on cutting speed, kerf width, total process time, MRR, surface roughness and amount of used wire. Ton is the most affecting factor for MRR and surface roughness increases when Ton increases [27]. P. Lakshmanan, et al. optimized the EDM processing attributes T_{on}, T_{off} & I by using the brass wire for the assessment of MRR on powder metallurgy route developed Magnesium-S_iC_p and flyash blended metallic composites. With an optimal current level of 8.5A, P_{on} of 700ms, and P_{off} of 200ms, the integrated Magnesium/S_iC_P-Flyash composites featuring metal matrix can remove the most material at a rate of 0.2296 g/min and tool usage at a rate of 0.0003 g/min. [31].

A. Mostafapor and H. Vahedi browsed during the processing of the magnesium alloy AZ91, the effects of three parameters used for input, encompassing pulse current, pulse on time and servo feed rate, has been explored. These functional metrics included substrate removal rate, kerf width, and the extent of surface roughness. Servo feed rate did not significantly affect process output characteristics, according to

ANOVA, although T_{on} & I_{pulse} did [32]. S. V. Bhaskar, T. R. Mohan surveyed and optimised machining constraints such as V, T_{off}, T_{on}, Wf rate & weight % of nano-SiC granules in WEDM of Mg metal matrix Nano-composites for measuring surface quality and MRR. Conclusions exhibited that the MRR measurements is significantly influenced by the pulse's voltage and time. When the voltage gains, the MRR value improves and the exterior quality rises at the same time [33].

2.0 Method selection & Material Processing

2.1 Preparation of Composite samples:

As per the literature review, Mg alloy AZ91 has been chosen as the base metal for the sample preparation. Table 01 depicts the contributors of AZ91 as obtained from supplier. Table 02 gives insights of mechanical attributes of base metal. The qualities significantly influence the extensive use of AZ91 in motor vehicle parts and engineering uses. Figure 01 and 02 shows the physical & chemical attributes of reinforcing materials (SiC and Al_2O_3) respectively.

Table-01 Contributors of AZ91

Element	Contribution (%)
Al	8.30%
Zn	1.0%
Mn	0.20%
Si	0.10%
Cu	0.03%
Fe	0.01%
Mg	Remaining

Table-02 Mechanical attributes of AZ91

Attributes	Values at Room
Density	1.81 gm/cm^3
Tensile	240-250 MPa
Yield Strength	160 MPa
Melting Point	421^{0}C
Purity	99.90%

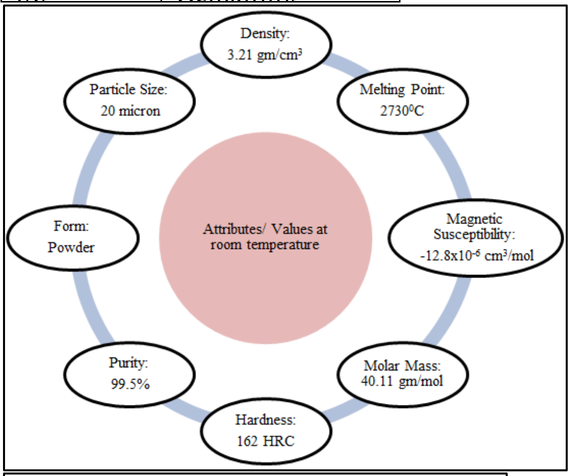

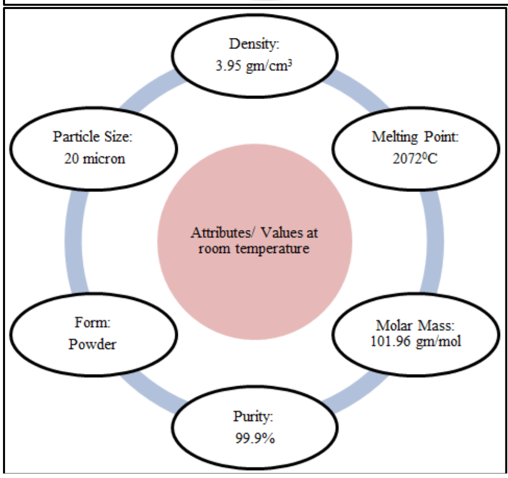

Fig.-01 Physical & Chemical qualities of SiC
Fig.-02 Physical & Chemical Properties of Al_2O_3

Mg alloy (AZ91) has been ground in tiny fragments by hexa cutting machine for compatibility of smelting. In-lab establishment of rotatory casting incorporating LPG fuelled smelter is created in institution facility. A SS410 steel bar with a circumference of 10 mm was utilised as a mixer. A tip was attached to a motor whereas the opposite side was designed with hexagonal form for turbulence production. Due to magnesium's high reactivity with the surroundings, an innocuous gas (argon) was employed to establish preventive covering against ambient oxygen in the air. Melted AZ91 is combined with warmed reinforcing material, S_iC-6% & Al_2O_3-3% by weight. Metallic mold was used to cast the specimens.

2.2 Processing Arrangement and Process Constraints

The entire processing of established $Mg/S_iC_p/Al_2O_{3p}$ blended metal matrix composites has been carried out on CNC WEDM, as displayed in figure 03 (a) & (b). Processing has been carried out using electrode made of molybdenum having dia of 0.18 mm and it has characteristics to be reusable. It has a 324MPa of tensile strength and 500MPa of shear strength with conductivity level (%IACS) of 34%. WEDM has an ultimate electrode speed of 10.4 meter/second. As a dielectric substance we utilised distilled water that was sold publicly. It serves as a channel for the processing of samples and clearing the fragments from slits.

Figure 03 (a) CNC WEDM Figure 03 (b) Processing of Specimen on setup

Input parameters for machining, T_{on}, T_{off}, I & WS have been altered along-with 03 diverse extents. All trials maintained constant values for numerous additional factors, including wire tension, dielectric medium concentration, cutting voltage, dielectric flow pressure and voltage variability. Table 03 depicts the processing factors along-with variability that are utilised while processing established composites.

Table 03: Utilised Processing factors along-with variations

Processing Factors	Variations/Levels		
	L1	L2	L3
Pulse-on-Time (T_{on})	6us	18us	30us
Pulse-off-Time (T_{off})	5us	7us	9us
Current (I)	1Amp.	3Amp.	5Amp.
Wire Speed (WS)	3.12m/sec.	6.76m/sec.	10.4m/sec.

2.3 Observations and Computations

Digital balancing device with accuracy of 0.1gram was employed to quantify proportionate value of true alloy AZ91 & reinforcing component prior meltdown. In developing the specimen 318.5gm (91%) of AZ91, 21gm (6%) of S_iC and 10.5gm (3%) of Al_2O_3 by weight was used. Processing duration of the specimen slit was captured from the equipment monitor in seconds. According to sample slit size, 40.248 mm^3 of Volume has been computed which is to be removed. The slit size has been remained unaltered while experimentations. Rate of Material removal (MRR) is assessed from equation 1.

$$\textbf{Material Removal Rate (MRR)} = \frac{\text{Volume of material removed from slot (mm3)}}{\text{Machining Time of slot (seconds)}} \ mm^3/Sec \quad ....(1)$$

Surface quality (R_a value) has been observed by surface quality tester supplied by Mitutoyo incorporating ISO grades. Factors including resolution, speed & measuring length have been held unchanged during entire observations. Three trials have been carried out for every specimen to optimise the measuring accuracy.

Figure 04(a)

Figure 04(b)

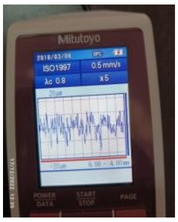

Figure 04(c)

Figure 04 (a), (b) & (c): Pictures taken during surface roughness measurement

3.0 RSM Based DoEs

A systematic method for organising, carrying out, and evaluating experiments to comprehend the connection between input variables (factors) and output variables (responses) is called Design of

Experiments (DoE). It's a methodical approach to data collection, analysis, and decision-making on procedures or goods. DoE assists in determining the elements that have a major influence on a desired result and their interrelationships. DoE is commonly of four types. 1) Full factorial design: Examines all combinations of factor levels. 2) Fractional factorial design: Examines a subset to reduce workload. 3) Response surface methodology (RSM): Explores complex relationships for optimization. 4) Taguchi methods: Focus on robustness and quality.

Response Surface Methodology (RSM) is a prevalent statistical approach employed for modelling and analysing issues when a response of significance is affected by multiple input factors. It facilitates the establishment of connections across output variables and machining parameters. Box–Behnken Design (BBD) & Central Composite Design (CCD) are two primary tests of design that RSM frequently uses. The BBD technique was used in the current work to create study inside the RSM context [34]. Employing the MINITAB-18 application, the test framework is developed considering the given input factors shown in Table 03. The BBD technique only needs three levels for every element and was developed for computing a quadratic system. N = 2k (k-1) + C0; is the total number of research tests (N) required by the RSM-BBD technique, where k is the count of input components and C0 is the count of central points required to preserve alignment and iso-variance [35-36]. Since there are four input parameters (k) and three central points (C0) in my study, there are 27 (R_{27}) planned experiments, as indicated in Table 04.

Table 04: DoEs for processing the specimen

Trial No.	T_{on} (Time- Pulse ON) (µs)	T_{off} (Time-Pulse OFF) (µs)	I (Current)	WS (Wire-Speed (m/sec.)
i	6	5	3	6.76
ii	30	5	3	6.76
iii	6	9	3	6.76
iv	30	9	3	6.76
v	18	7	1	3.12
vi	18	7	5	3.12
vii	18	7	1	10.40
viii	18	7	5	10.40
ix	6	7	3	3.12
x	30	7	3	3.12
xi	6	7	3	10.40
xii	30	7	3	10.40
xiii	18	5	1	6.76
xiv	18	9	1	6.76
xv	18	5	5	6.76
xvi	18	9	5	6.76
xvii	6	7	1	6.76
xviii	30	7	1	6.76
xix	6	7	5	6.76
xx	30	7	5	6.76
xxi	18	5	3	3.12
xxii	18	9	3	3.12
xxiii	18	5	3	10.40
xxiv	18	9	3	10.40
xxv	18	7	3	6.76
xxvi	18	7	3	6.76
xxvii	18	7	3	6.76

In the present study, the machining process was systematically conducted using DoE methodology to investigate the impact of key process attributes on the machining performance. By employing a structured experimental design, relevant input attributes like wire speed, I, T_{on} and T_{off} were varied according to a predefined DoE matrix. The specimens have been processed on computer numeric controlled wire EDM employing the DoEs information provided in table 04. The findings obtained throughout the EDM processing are displayed in table 05 below.

Table 05: Findings during processing of Specimens

Trial No.	Processing Duration (Sec.)	Trial No.	Processing Duration (Sec.)	Trial No.	Processing Duration (Sec.)
i	318	x	459	xix	317
ii	320	xi	255	xx	318
iii	323	xii	256	xxi	460

iv	322	xiii	321	xxii	457
v	466	xiv	358	xxiii	256
vi	457	xv	319	xxiv	257
vii	449	xvi	320	xxv	319
viii	435	xvii	400	xxvi	316
ix	457	xviii	326	xxvii	317

4.0Results and Discussion

Prepared samples of $AZ91/SiC_p/Al_2O_{3p}$ blended composites were processed on Wire cut EDM in accordance with DoE acquired by way of RSM-BBD perspective. The computations of the extent of surface quality (R_a) and machining rate (MRR) based on findings obtained while the processing is displayed in Table 06 below.

Table 06: Findings of R_a & MRR

Trial No.	Metal Removal Rate (MRR) (mm3/Second)	Surface Roughness (R_a- microns) (µm)	Trial No.	Metal Removal Rate (MRR) (mm3/Second)	Surface Roughness (R_a- microns) (µm)
i	0.126566038	04.273	xv	0.126969279	06.279
ii	0.127075000	08.428	xvi	0.125775000	07.967
iii	0.126606811	04.197	xvii	0.100620000	02.958
iv	0.126593789	08.813	xviii	0.123460123	07.196
v	0.078369099	06.294	xix	0.126965300	05.347
vi	0.088070022	08.618	xx	0.128566038	09.185
vii	0.164639198	04.984	xxi	0.089495652	07.310
viii	0.162524138	06.154	xxii	0.098070022	05.869
ix	0.088070022	04.218	xxiii	0.159118750	05.934
x	0.087686275	08.784	xxiv	0.157607004	05.198
xi	0.157835294	04.356	xxv	0.126169279	06.034
xii	0.158218750	07.108	xxvi	0.129367089	07.109
xiii	0.126383178	04.427	xxvii	0.129965300	06.857
xiv	0.112824581	05.043	-----	-----	-----

4.1RSM Models for developed specimen

The RSM technique was used to formulate statistical predictions for the levels of surface roughness and material removal rate when processing blended composites utilising molybdenum electrode. The regression models for the compiled MRR and R_a are presented by equations 2 & 3 respectively.

Statistical model for rate of metal removal

$MRR = 0.0100 + 0.00163\, T_{on} - 0.00009\, T_{off} + 0.01067\, I + 0.01515\, WS - 0.000022\, T_{on} \times T_{on} - 0.000009\, T_{off} \times T_{off} - 0.001194\, I \times I - 0.000129\, WS \times WS - 0.000005\, T_{on} \times T_{off} - 0.000221\, T_{on} \times I + 0.000004\, T_{on} \times WS + 0.000773\, T_{off} \times I - 0.000346\, T_{off} \times WS - 0.000406\, I \times WS$

.... (2)

Equation 02 is a multiple regression model predicting the response variable MRR based on four predictor variables: T_{on}, T_{off}, I, and WS. The equation also includes quadratic terms and interaction terms. The expected value of MRR when all predictor variables are zero intercepted as 0.01. Each coefficient (e.g., 0.00163 for T_{on}) indicates the change in MRR for a one-unit increase in that variable, holding other variables constant.

Table 07: Analysis of variance for MRR

Factor/ Source	Degree of	Sequential sum of	Contribution	Adjusted Sum of	Adjusted Mean	F-Statisti	Significance Level (P-
Regression	14	0.016081	97.60%	0.016081	0.001149	34.84	0.000
Linear	4	0.015709	95.34%	0.015709	0.003927	119.12	0.000
T_{on}	1	0.000052	0.31%	0.000052	0.000052	1.57	0.234
T_{off}	1	0.000006	0.03%	0.000006	0.000006	0.17	0.690
I	1	0.000230	1.40%	0.000230	0.000230	6.99	0.021
WS	1	0.015421	93.60%	0.015421	0.015421	467.76	0.000
Square	4	0.000160	0.97%	0.000160	0.000040	1.22	0.355
T_{on} x T_{on}	1	0.000022	0.14%	0.000053	0.000053	1.59	0.231
T_{off} x T_{off}	1	0.000016	0.10%	0.000000	0.000000	0.00	0.989
I x I	1	0.000106	0.64%	0.000122	0.000122	3.69	0.079
WS x WS	1	0.000016	0.09%	0.000016	0.000016	0.47	0.505
2-Way	6	0.000212	1.28%	0.000212	0.000035	1.07	0.432

T_{on} x T_{off}	1	0.000000	0.00%	0.000000	0.000000	0.00	0.964
T_{on} x I	1	0.000113	0.68%	0.000113	0.000113	3.42	**0.089**
T_{on} x WS	1	0.000000	0.00%	0.000000	0.000000	0.00	0.948
T_{off} x I	1	0.000038	0.23%	0.000038	0.000038	1.16	0.303
T_{off} x WS	1	0.000025	0.15%	0.000025	0.000025	0.77	0.397
I x WS	1	0.000035	0.21%	0.000035	0.000035	1.06	0.324
Residual	12	0.000396	2.40%	0.000396	0.000033		
Model Misfit	10	0.000387	2.35%	0.000387	0.000039	9.30	0.101
Experimental	2	0.000008	0.05%	0.000008	0.000004		
Overall	26	0.016476	100.00%				

Table 08: Model summary for rate of metal removal

Residual Standard Deviation (S)	Coefficient of Determination (R-	Adjusted R-squared	Predicted Residual Error Sum of Squares	Predicted R-squared
0.0057418	97.60%	94.80%	0.0022495	86.35%

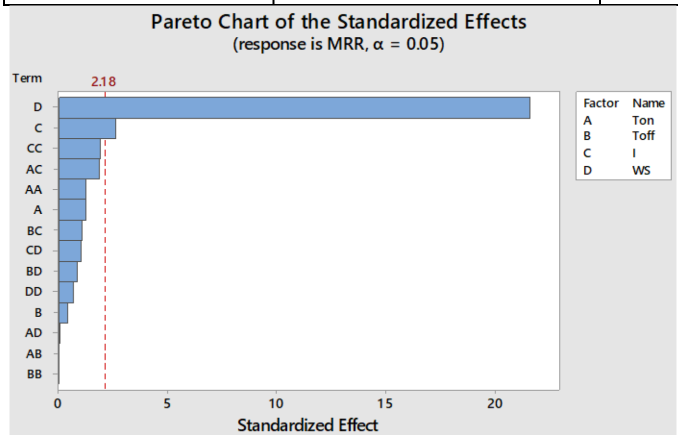

Figure 05: Effects of Pareto for rate of metal removal

Table 07 displays the ANOVA for the MRR that occurs while the specimen machining. The model explains 97.60% of the variance in MRR with a very high F-value (34.84) and a significance level of 0.000. This conveys that model is mathematically relevant. WS (Wire Speed) is most significant contributor (93.60% of the total model), with a highly significant p-value (0.000). It has a strong positive effect on MRR. I (Current) also shows a significant effect (p = 0.021), contributing 1.40% to the model. T_{on} and T_{off} factors are less relevant (p-values of 0.234 & 0.690 respectively), indicating these factors does not create a meaningful influence on MRR in present study. Figure 05 displays Pareto Bar Graph of the standardised influence on MRR, which illustrates important factors and their interactions.

Statistical model for Ra:

$$Ra = -1.57 + 0.262\,T_{on} + 0.69\,T_{off} + 0.750\,I + 0.157\,WS - 0.00126\,T_{on}*T_{on} - 0.0805\,T_{off}*T_{off} - 0.0582\,I*I - 0.0140\,WS*WS + 0.0048\,T_{on}*T_{off} - 0.0042\,T_{on}*I - 0.01038\,T_{on}*WS + 0.0670\,T_{off}*I + 0.0242\,T_{off}*WS - 0.0396\,I*WS \quad \ldots\ldots\ldots\ldots\ldots (3)$$

Equation 03 is a multiple regression model predicting the response variable R_a based on four predictor variables: T_{on}, T_{off}, I, and WS. The equation also includes quadratic terms and interaction terms. The expected value of R_a when all predictor variables are zero intercepted as -1.57. A one-unit increase in T_{on} results in an increase of R_a by 0.262, T_{off} leads to an increase of 0.69 in R_a, Increasing the current I by one unit raises R_a by 0.750 & A one-unit increase in WS increases R_a by 0.157 holding all other variables constant.

Table 09: Analysis of variance for R_a

Factor/	**Degree**	**Sequential**	**Contribut**	**Adjusted**	**Adjusted**	**F-**	**Significance**
Regression	14	68.8508	92.98%	68.8508	4.9179	11.35	**0.000**
Linear	4	66.5220	89.84%	66.5220	16.6305	38.39	0.000
T_{on}	1	48.6623	65.72%	48.6623	48.6623	112.34	**0.000**
T_{off}	1	0.0158	0.02%	0.0158	0.0158	0.04	0.852
I	1	13.3310	18.00%	13.3310	13.3310	30.78	**0.000**
WS	1	4.5129	6.09%	4.5129	4.5129	10.42	**0.007**
Square	4	0.6686	0.90%	0.6686	0.1671	0.39	0.815

International Journal of Environmental Sciences
ISSN: 2229-7359
Vol. 11 No. 21s, 2025
https://theaspd.com/index.php

$T_{on} \times T_{on}$	1	0.0074	0.01%	0.1753	0.1753	0.40	0.537
$T_{off} \times T_{off}$	1	0.3022	0.41%	0.5527	0.5527	1.28	0.281
I x I	1	0.1749	0.24%	0.2887	0.2887	0.67	0.430
WS x WS	1	0.1841	0.25%	0.1841	0.1841	0.43	0.527
2-Way	6	1.6603	2.24%	1.6603	0.2767	0.64	0.698
$T_{on} \times T_{off}$	1	0.0531	0.07%	0.0531	0.0531	0.12	0.732
T_{on} x I	1	0.0400	0.05%	0.0400	0.0400	0.09	0.766
T_{on} x WS	1	0.8226	1.11%	0.8226	0.8226	1.90	0.193
T_{off} x I	1	0.2873	0.39%	0.2873	0.2873	0.66	0.431
T_{off} x WS	1	0.1243	0.17%	0.1243	0.1243	0.29	0.602
I x WS	1	0.3329	0.45%	0.3329	0.3329	0.77	0.398
Residual	12	5.1980	7.02%	5.1980	0.4332		
Model Misfit	10	4.5658	6.17%	4.5658	0.4566	1.44	0.477
Experimental	2	0.6322	0.85%	0.6322	0.3161		
Overall	26	74.0488	100.00%				

Table 10: Regression Model conclusion for R_a

Residual Standard	Coefficient of Determination (R-	Adjusted R-	Predicted Residual Error Sum of Squares	Predicted R-squared
0.658151	92.98%	84.79%	27.7214	62.56%

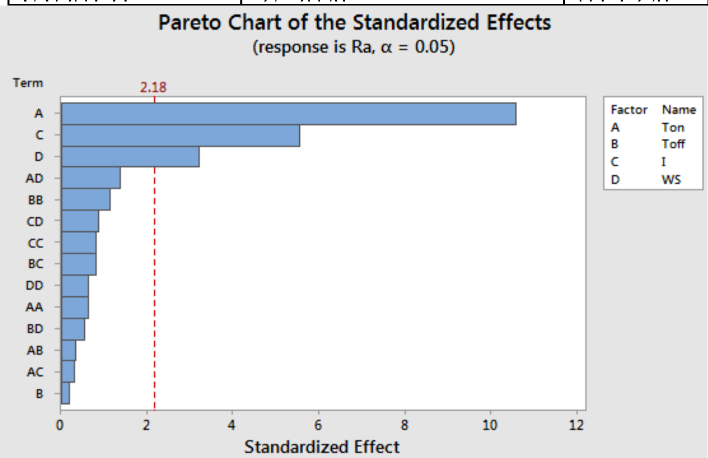

Figure 06: Effects of Pareto for R_a

The confidence level, which in this case is 95%, serves as the foundation for the model's adequacy. When the significance level is lesser than 0.05, the attributes and interactions will be deemed influential. ANOVA for surface roughness (R_a) is shown in Table 09. Having an influential F-statistics value of 11.35 and significance level of 0.000, the model captures 92.98% of the R_a variability. This suggests that the model is mathematically effective overall. Ton is the best driver of Ra, as evidenced by its enormous impact (65.72%) and incredibly influential p-value (0.000). I also significantly influences Ra, contributing 18.00% and showing significance (p = 0.000). WS contributes 6.09% and is significant (p = 0.007), indicating it positively impacts Ra. T_{off} has a very small contribution (0.02%) and is not significant (p = 0.852). The R_a model summary is displayed in Table 10. By providing larger R-sq and R-sq(adj) values and a lesser quantity of S, it argues that the model is adequate.

4.2Analysing output responses

The processed composite's output attributes are assessed using predetermined input variables. Using the RSM-BBD technique, the impact of input factors on the machining rate (MRR) & extent of R_a (surface quality) is portrayed using Minitab-18.

Figure 7(a) & 7(b) depicts the influence of current and wire speed on MRR by employing RSM-BBD technique. Figure 7(c) demonstrates cumulative influence of T_{on} & I at T_{off} =7µs & WS = 6.76m/sec on MRR.

The MRR has been observed growing by 26.18% when the current is increased from low to high at T_{on} = 6µs & WS = 6.76 m/sec, but MRR grows by 41.35% at T_{on} = 30µs. MRR rises by 22.8% if we raise the T_{on} from 6µs to 30µs for minimal current, while it little changes at larger current values. The RSM graph also shows that the maximum MRR in the current investigation is produced by higher current with a small pulse-on-time. The RSM graphs in figures 7(a) and 7(b) further support the ANOVA table 07's finding that current and wire speed have a major effect on MRR. Graph depicts the relevant effects of I and WS on rate of metal removal.

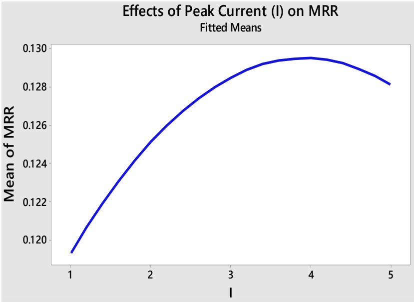

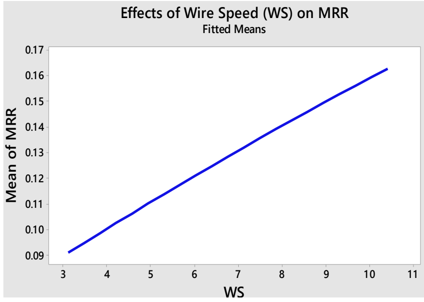

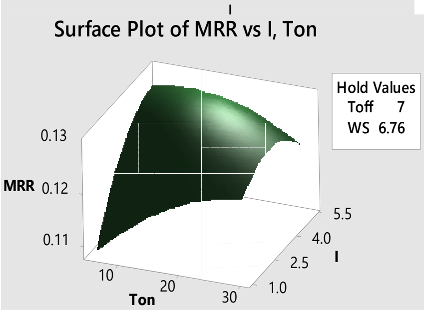

Figure 7(a):Current's effect on MRR Figure 7(b):WS's effect on MRR Figure 7(c): Cumulative effect of I & T_{on} on MRR

Using MINITAB-18 software, the correlation between R_a and input factors is shown, as seen in figure 08 (a-d). Individual factors' effects on R_a have been demonstrated to be noteworthy in ANOVA table 09, and the graphs generated via the RSM-BBD technique make this evident. For T_{on}, I, and WS, respectively, figures 08(a), (b), & (c) illustrate the influence on R_a.

Figure 08(d) illustrates the combined impact of WS and T_{on} at T_{off} = 7μs & I = 3A on the surface quality of the processed blended composite specimen. The R_a level is shown to rise 1.08 times when the T_{on} is increased from low to high at a WS of 3.12 meter/second, while it grows 0.63 times when the WS is increased to 10.4 meter/second. R_a level dropped to 0.19 percent as WS rises from low to high at T_{on} = 30μs, whereas Ra value changes nominally at T_{on} = 6μs. Figure 7(d)'s combination graph for the R_a level shows a similar representation.

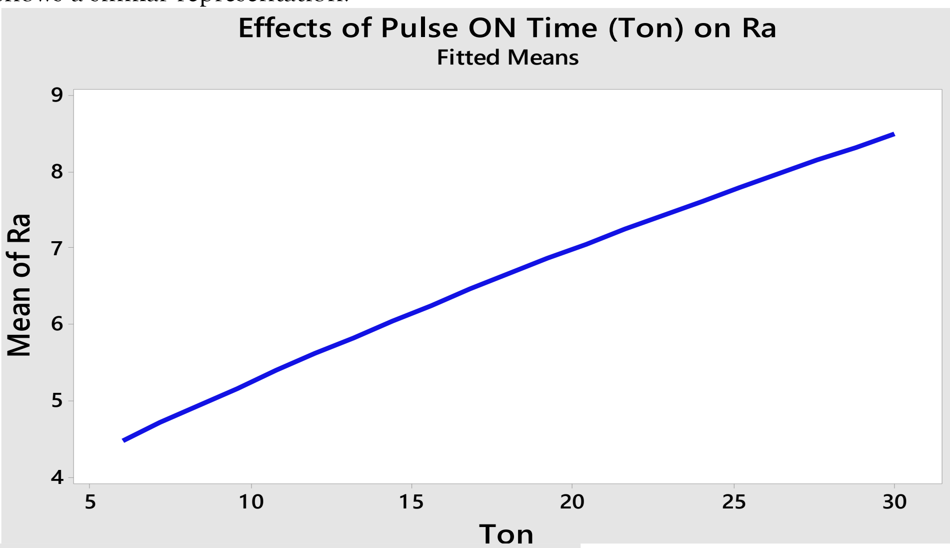

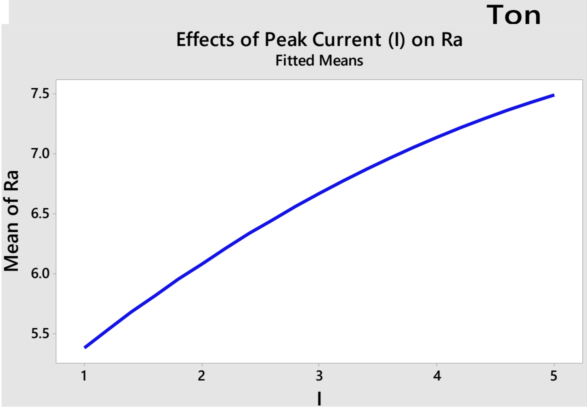

Figure 08(a): Graph depicting T_{on}'s effect on R_a Figure 08(b): Graph depicting I's effect on R_a

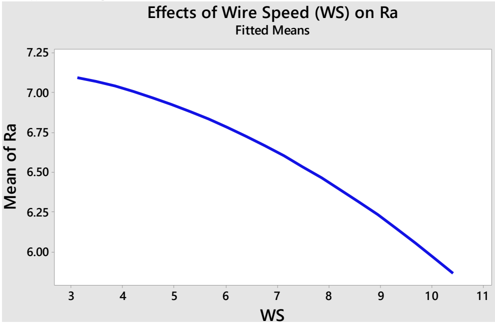

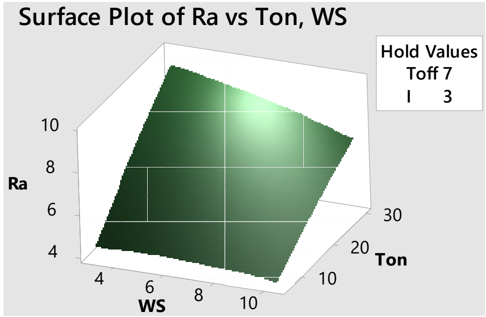

Figure 08(c): Graph depicting WS's on R_a Figure 08(d): Cumulative influence of Wire Speed & T_{on} on R_a

4.3Multi Objective Optimization

The RSM's BBD framework was utilised for establishing trials. Composite desirability (CD) approach of experimental design has been utilised to get most effective and optimal result along-with combination of entry variables during wire cut machining of magnesium centered composites. Typically, CD strategy may be employed to improve machining operations with nonlinear behaviour across many targets. Based on the optimal balance of input factors, this method provides the best desired output responses. Greater MRR values are preferable for material removal rates, but lesser R_a values are preferable for surface quality. The variables taken into account to get the best result for the input factors are displayed in Table 11. Table 12 displays the input variable optimisation utilising the composite desirability technique of RSM.

Table 11: Attributes for optimal responses

Output	Objecti	Min.	Desired	Max	Sensitivity	Significance
R_a	Lower		02.95800	09.185	1.0	1.0
MR Rate	Higher	0.078369	0.16464		1.0	1.0

Table 12: Optimum result for input factors

Response	T_{on}	T_{off}	Current	Wire speed	R_a Fit	MR Rate	Overall Desirability
i	6µs	5µs	1.20202A	10.4m/sec	2.98165	0.153128	0.929124

Table 13: Multiple result forecasting for outputs and the inputs

Variable	T_{on}	T_{off}	I	Wire speed
Setting	6 µs	5 µs	1.20202 A	10.4m/sec

Responses	Fit	Standard Error Fit	95% Confidence Interval	95% Prediction Interval
R_a	2.982	0.954	(0.903, 5.060)	(0.457, 5.507)
MR Rate	0.15313	0.00832	(0.13500, 0.17126)	(0.13110, 0.17516)

The ideal settings for wire EDM of Mg-based blended composite augmented together with SiC and Al_2O_3 utilising the molybdenum electrode is displayed in figure 09 below. Using the composite-desirability of RSM, an optimised graph for the input variables was created using Minitab-18 software.

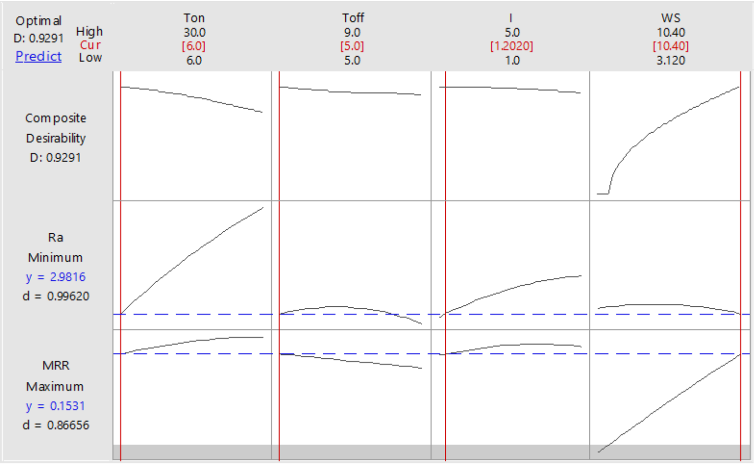

Figure 09: Multi objective optimization graph using Composite Desirability approach

4.4 Verifying trial for multi objective optimization

Table 14 shows the results of a validation test that was conducted in relation to the optimised input components obtained using the CD technique of RSM as per table 12. With reference to Table 17, it can be inferred that the confirming outcome yields a greater value of R_a, which explains the subpar surface quality, than the anticipated value, and a larger MRR at the optimum blend of input variables obtained by the CD technique.

Table 14: Outcomes of Validating Test

Exp	T_{on}	T_{off}	I	WS	Ideal forecasting values		Validation Test outputs	
					R	MRR	R	MRR
i	6µ	5µ	1.20202	10.4m/se	2.98165	0.153128	3.05711	0.159508

5.0 Summary and Extended scope

The current study concentrated on creating a blended composite composed of the magnesium alloy AZ91, employing SiC powder and Al_2O_3 as reinforcing materials. The RSM-BBD technique has created design experiments for outputs on Minitab 18 software for wire EDM machining using molybdenum electrode. To find the best solution, multifaceted optimisation has been done using the composite desirability (CD) technique. The key points that follow can be enumerated in support of the study's findings:

i. Using two powdered reinforcements, Al_2O_3 and SiC, blended composites have been effectively created using the stir casting process.

ii. Second order regression models were developed using the RSM-BBD technique to determine how input factors like T_{on}, T_{off}, I, and WS affected the MRR and SR outcome values. The models that have been constructed are sufficient.

iii. ANOVA shows that the interaction across I x I and T_{on} x I has a significant impact on MRR while the machining of blended composite on wire EDM. The best factors for MRR are current and wire speed.

iv. According to ANOVA, the most important criteria for achieving improved surface finish are WS, T_{on} & I.

v. Rising the level of applying current from 1A to 5A at T_{on} = 6µs increases the MRR by 26.18% while it increases by 41.35% at greater T_{on}. Greater amount of MRR (0.164639198 mm^3/sec) has been acquired at T_{on}=18µs, T_{off}=7µs, I=1A & WS=10.40m/sec. The value I=1A was crucial in achieving a higher MRR.

vi. R_a rises by 0.63 folds at superior wire speeds, whilst surface roughness improves by 1.08 folds when T_{on} increased from lower to higher, while maintaining WS at 3.12m/sec. Better surface quality may be achieved with reduced input factors. The values of T_{on}=6µs, T_{off}=7µs, I=1A, and WS=6.76m/sec yield a lesser value of surface roughness (R_a = 2.958µm).

vii. For multi-objective optimisation, the DoE-based RSM-CD technique shows a mixture of ideal input variables. T_{on}=6µs, T_{off}=5µs, I=1.2A & WS=10.4m/sec for minimal R_a of 2.98165µm and strong MRR of 0.153128 mm^3/sec.

viii. The present investigation concludes that wire speed, a contributing variable, was critical in processing a blend of materials based on magnesium alloy AZ91 in order to achieve greater metal removal rates and improved surface quality.

Recognition: Author desires to recognize FoME, IoT, SRMU, Lucknow for providing registration number 202010102000001.

Author's Contribution: Dheeraj Kumar- Setup development, Experimentation, Resources, Conceptualization, Validation, Information Gathering, Drafting paper; **Rajesh Kumar Porwal-** Guidance, content review & revision.

REFERENCES

1. Kumar, Dheeraj, and Rajesh Kumar Porwal. "Recent Advances in Machining of Composite Materials by Electrical Discharge Machine." Key Engineering Materials 965 (2023): 3-20. DOI:10.4028/p-TsFf0o.
2. Kumar, D., Porwal, R.K. Parametric Optimization of Thermoelectric Machining of Stir-Cast Hybrid Magnesium Metal Matrix Composite with Alumina and Silicon Carbide as Reinforcement. J. Inst. Eng. India Ser. D 105, 1927–1943 (2024). https://doi.org/10.1007/s40033-023-00628-x.
3. D. Zolotova, V. Serpova, M. Prokofiev, L. Rabinskiy and A. Shavnev, A study of the composition and microstructure of aluminum matrix composites reinforced with alumina fibers. IOP Conf. Series: Materials Science and Engineering 124 (2016) pp. 012-0135. doi:10.1088/1757-899X/124/1/012135.
4. M. K. Surappa, Aluminium matrix composites: Challenges and opportunities. Sadhana Vol. 28, Parts 1 & 2, February/April (2003) 319–334. https://doi.org/10.1007/BF02717141
5. D. P. Singh, S. Mishra, S. K. S Yadav, R. K. Porwal and V. Singh, Comparative analysis and optimization of thermoelectric machining of alumina and silicon carbide reinforced aluminum metal matrix composites using different electrodes. Journal of Advanced Manufacturing Systems, doi: 10.1142/S0219686723500191, pp 1-29, 2023.
6. Anil Kumar, S. Kumar, N. K. Mukhopadhyay, Introduction to magnesium alloy processing technology and development of low cost stir casting process for magnesium alloy and its composites. Journal of magnesium and alloys 6 (2018) pp. 245-254. https://doi.org/10.1016/j.jma.2018.05.006
7. A.I. Taub , P.E. Krajewski , A.A. Luo , J.N. Owens, The evolution of technology for materials processing over the last 50 years: The automotive example, J. Metals 59 (2) (2007) 48–57. https://doi.org/10.1007/s11837-007-0022-7
8. A.A. Luo , Applications: aerospace, automotive and other structural applications of magnesium, Fundamentals of Magnesium Alloy Metal- lurgy, Woodhead Publishing Ltd, Cambridge, UK, 2012, pp. 393–426. Chapter 8.
9. K.U. Kainer, Magnesium-Alloys and Technologies, Wiley-VCH, Wein- heim, Germany, 2003.
10. A.A. Luo, Magnesium: Current and potential automotive applications, J. Metals 54 (2) (2002) 42–48. https://doi.org/10.1007/BF02701073.
11. H.-H. Becker, Status, potential & challenges for automotive magnesium applications from the point of view of an OEM, in: Proceedings of the Sixty-fifth Annual World Magnesium Conference, May 18–20, Warsaw, Poland, 2008.
12. Y. Michiura, Current magnesium research & application in automotive industry in Japan, in: Proceedings of the International Automotive Body Congress, November 7–8, Troy, MI, USA.
13. J.S. Balzer, P.K. Dellock, M.H. Maj, G.S. Cole, D. Reed, T. Davis, T. Lawson, G. Simonds, Structural magnesium front end support. SAE Technical Paper 2003-01-0185, SAE International, Warrendale, PA, 2003.
14. M. Hoeschl, W. Wagener, J. Wolf, BMW's magnesium–aluminium composite crankcase, state-of-the-art light metal casting and manufactur- ing. SAE Technical Paper 2006-01-0069, SAE International, Warrendale, PA, 2006.
15. Kumar, Anil, Santosh Kumar, and N. K. Mukhopadhyay. "Synthesis and Characterization of SiCp Reinforced Magnesium Alloy Based Metal Matrix Composite Through Vacuum Assisted Stir Casting Process." International Journal of Applied Engineering Research 12.24 (2017): 16087-16093.
16. B. L. Mordike and T. Ebert, "Magnesium Properties - applications - potential," Mater. Sci. Eng. A, vol. 302, no. 1, pp. 37–45, 2001.
17. K. Ponappa, S. Aravindan, and P. V. Rao, "Influence of Y 2 O 3 particles on mechanical properties of magnesium and magnesium alloy (AZ91D)," J. Compos. Mater., vol. 47, no. 10, pp. 1231–1239, 2013.
18. K. Ponappa, S. Aravindan, and P. V. Rao, "Grinding of magnesium /Y 2 O 3 metal matrix composites," Proc. Inst. Mech. Eng. Part B J. Eng. Manuf., vol. 226, no. 10, pp. 1675–1683, 2012.
19. L. Lu, K. K. Thong, and M. Gupta, "Mg-based composite reinforced by Mg2Si," Compos. Sci. Technol., vol. 63, no. 5, pp. 627–632, 2003.
20. X. Zhang, Q. Zhang, and H. Hu, "Tensile behaviour and microstructure of magnesium AM60-based hybrid composite containing Al2O3 fibres and particles," Mater. Sci. Eng. A, vol. 607, pp. 269–276, 2014.
21. D. Lu, Y. Jiang, and R. Zhou, "Wear performance of nano-Al2O3 particles and CNTs reinforced magnesium matrix composites by friction stir processing," Wear, vol. 305, no. 1–2, pp. 286–290, 2013.
22. M. Paramsothy, X. H. Tan, J. Chan, R. Kwok, and M. Gupta, "Al2O3 nanoparticle addition to concentrated magnesium alloy AZ81: Enhanced ductility," J. Alloys Compd., vol. 545, pp. 12–18, 2012.
23. H. Ferkel and B. L. Mordike, "Magnesium strengthened by SiC nanoparticles," Mater. Sci. Eng. A, vol. 298, no. 1–2, pp. 193–199, 2001.
24. I. Balasubramanian, R. Maheshwaran, V. Manikanadan, Nilesh Patil, M. A. Raja and R. M. Singari, Mechanical characterization and machining of squeeze cast AZ91D/SiC magnesium based metal matrix composite. Procedia manufacturing 20 (2018) pp 97-105.
25. V. Kavimani, K. S. Prakash, T. Thankachan, Multi-objective optimization in WEDM process of graphene-SiC-magnesium composite through hybrid techniques. Measurement 145 (2019) pp. 335-349.
26. L. Arunkumar, B. K. Raghunath, Electro Discharge Machining Characteristics of Mg/SiCP Metal matrix composites by Powder Metallurgy (P/M) Techniques. International Journal of Engineering and Technology (IJET), (ISSN 0975-4024), Vol. 5 No. 5 Oct-Nov 2013, pp 4332-4338.
27. P. M. Gopal, K. S. Prakash & S. Jayaraj, WEDM of Mg/CRT/BN Composites: Effect of Materials and Machining Parameters. Materials and manufacturing processes, Vol. 33, 2018 issue 1, pp. 77-84

28. J. Tapadar, Raj Thakur, P. Chetia, S.K. Tamang, S. Samanta, modeling of WEDM parameters while machining Mg-SiC metal matrix composite. International Journal of Technology (2017) vol. 5, pp. 878-886.
29. Ravindranadh Bobbili, V. Madhu, A.K. Gogia, Multi response optimization of wire-EDM process parameters of ballistic grade aluminium alloy. Engineering Science and Technology an International Journal, 18 (2015), pp. 720-726.
30. Wire Selection, Last access: 10/04/2023, https://www.novotec-edm.com/wire-selection.
31. Kalyani S. Kanekar, Diwesh B. Meshram, Investigation and Optimization of EDM performance measures using empirical data analysis, International Journal of Research in Engineering and Technology, vol. 04, issue 08, 2015, pp. 213-223.
32. Jaber E. Abu Qudeiri, Aiman Zaiout, Abdel-Hamid I. Mourad, Mustufa Haider Abidi and Ahmed Elkaseer, Principles and Characteristics of Different EDM Processes in Machining Tool and Die Steels. Appl. Sci. 2020, 10, 2082; doi: 10.3390.
33. Poovazhagan Lakshmanan, G. Kumanan, L. Arunkumar, S.C. Amith, Experimental investigations of material removal rate on Mg/SiCp-flyash hybrid metal matrix composites by electrical discharge machining. Materials Today: Proceedings 46 (2021) pp. 986–990.
34. Amir Mostafapor and Hossein Vahedi, Wire electrical discharge machining of AZ91 magnesium alloy; investigation of effect of process input parameters on performance characteristics. Eng. Res. Express 1 (2019) 015005. https://doi.org/10.1088/2631-8695/ab26c8.
35. S. Vijayabhaskar, T. Rajmohan, Experimental Investigation and Optimization of Machining Parameters in WEDM of Nano-SiC Particles Reinforced Magnesium Matrix Composites. Silicon, volume 11, pages1701–1716 (2019).
36. C. Kuo, C. Yao Hsu, J. H. Chen and P. W. Lee, Discharge current effect on machining characteristics and mechanical properties of Aluminium alloy 6061 workpiece produced by electric discharge machining process, Advances in Mechanical Engineering, vol 9 (11), pp. 1-8 (2017).
37. X. Li, W. Hou, B. Han, L.Xu, Z. Li, P. Nan, X. Ni, Investigation on the continuous wave mode and the ms pulse mode fibre laser drilling mechanisms of the carbon fibre reinforced composite, Polymers 12, 706 (2020). doi: 10.3390/polym12030706.
38. S. Mullick, A. Agarwal, A. Nath, Effect of laser incidence angle on cut quality of 4 mm thick stainless steel sheet using fibre laser, Optics and Laser Technology, 81 (2016), pp. 168-179.